Benha Journal of Applied Sciences (BJAS) **print: ISSN 2356–9751**
Vol. (8) Issue (5) (2023), (277-284) **online: ISSN 2356–976x**
http://bjas.journals.ekb.eg

An Experimental Investigation on Machining of 90W-7Ni-3Fe Alloys Using Wire Electrical Discharge Machining

Bassem A. Mohamed, Saleh H. Kaytbay
Department of Mechanical Engineering, Benha Faculty of Engineering, Benha University, Egypt.
Corresponding author: bassemahmed229@gmail.com

Abstract

Tungsten heavy alloys (WHAs) are desired in many applications, including gyroscope rotors for aerospace and spacecraft, die-casting molds, and shielding elements for radiation protection. Owing to their superior physical, chemical, and mechanical characteristics, which as high density, great radiation shielding capability, high strength, low thermal expansion, high anti-impact toughness, and good corrosion resistance. However, such applications require highly precise complex geometries. Cutting WHAs using conventional machining processes is challenging due traditional machining processes of WHAs can present problems, obtaining high-precision parts, such as the challenge of getting high accuracy and tight tolerances. Due to WHAs' high toughness, tools wear out quickly and break. For manufacturers, this means higher expenses and more work. Additionally, traditional machining methods' high heat generation causes thermal distortion of the machined component and can reduce the life of the cutting tool. In this paper, Wire Electrical discharge machining (WEDM) is utilized for investigating the machinability of heavy tungsten alloys with a composition of 90W7Ni3Fe. Half factorial design of the experiment was conducted to investigate the effect of machining variables on the material removal rate. The variables include arc-on time (AON), arc-off time (AOF), open voltage (OV), feed rate (FR), servo voltage (SV), and wire tension (WT). An additional ANOVA test was conducted to investigate the significant effect of each variable. The results showed that (FR) has the highest impact on MRR, followed by (SV), (OV) and (AON) which in turn enhance the surface quality. A regression model was developed for predicting the MRR with an accuracy of 90.37%.

Keywords: 90W7Ni3Fe, WHAs, WEDM, MRR, Half factorial.

1. Introduction

90W-7Ni-3Fe Tungsten Heavy Alloys (WHAs) are high-density materials that are fabricated from the elemental powders of tungsten (W), nickel (Ni), and iron (Fe) [1]. These alloys are renowned for their superior mechanical properties, including high strength, toughness, and hardness. Due to these properties, WHAs are used in applications that demand high-density materials, including radiation shielding, aerospace, defense, and medical technologies. Additionally, it is a vital material in thin film technology owing to its low coefficient of thermal expansion and a high degree of electrical conductivity. Due to its low cost, it serves as a connecting material in integrated circuits [2]. One of the main challenges associated with WHAs is their brittleness. Additionally, their high density and hardness can make them challenging to machine or weld [3]. Traditional machining processes of WHAs can present problems, including difficulty in achieving high accuracy and tight tolerances, which can be a barrier to achieving high-precision parts. The high toughness of WHAs leads to rapid tool wear, and breakage occurs. Which in turn increases costs and is time-consuming for manufacturers [4]. Moreover, high heat generation in Traditional machining processes leads to thermal distortion of the machined component and can also affect the life of the cutting tool [5]. Moreover, achieving a high-quality surface finish is challenging due to its uneven and rough surfaces [6]. Overall, traditional machining processes of WHAs can be complex, costly, and time-consuming. In contrast, wire electrical discharge machining offers several advantages compared to traditional machining [7], as the process uses a thin, electrically charged wire guided by a computer-controlled program to precisely cut through the material without requiring physical contact between the wire and the workpiece, as an electrode that generates sparks to erode the workpiece [8]. The wire is continuously fed into the workpiece, and as the electrode spark jumps across the gap, it erodes the material [9]. The material is removed in WEDM through melting and vaporization by an electric spark discharge produced by pulsating direct current power between electrodes [10]. With WEDM, the workpiece is the positive electrode, while the negative electrode is a wire constantly moving. Under the action of the dielectric liquid, sparks form between two electrodes that are positioned closely together [11]. Due to its low viscosity and quick cooling rate, water is used as the dielectric in WEDM [12]. The spark energy from the wire is controlled to produce a precise cut in the workpiece, resulting in high dimensional accuracy. Therefore, this study aims to investigate the effects of various process parameters on the WEDM of this alloy and to optimize the process parameters to

achieve the desired machining performance, material removal rate, and surface finish. The variables include arc-on time (AON), arc-off time (AOF), open voltage (OV), feed rate (FR), servo voltage (SV), and wire tension (WT) [13]. A half-factorial design can be used to analyze the machining parameters for WEDM. Because full factorial increases the number of experiments and costs, half-factorial design has favored over full factorial design. Nonetheless, half-factorial designs are among the most popular since they offer adequate details on main effects and low-order interactions. This statistical method involves manipulating certain variables to test their effects on the machining process. By testing only half of the possible combinations, the process can be streamlined while providing sufficient data to analyze the results. This can help to identify the optimal machining parameters for a given material, allowing for more efficient and effective machining [11]. The major purpose of this study was to conduct experimental investigations of the effects of WEDM process parameters (AON - AOFF - OV - FR - SV - WT) on the material removal rate of heavy tungsten alloys by half-factorial design.

2. EXPERIMENTAL SETUP

The experiment is performed using a wire EDM machine Fig.1, and the formation material is 90W7Ni3Fe with a density of 17.15 (gm/cc) sample diameter of 16 mm. The specifications for the machine are listed in Table 1. The trials will be acted upon as planned on MINITAB. With six input parameters and a half-factorial design of two levels, 32 experiments are produced. Material removal rate has been measured using Eq. (1) for all the experimental conditions. The regulating input parameters include Arc one time, Arc Off time, Open voltage, Feed Rate, Servo voltage, and Wire tension. Table 2 show WEDM parameters and their levels. Selecting the range of input parameters is aided by pilot trials.

Table 1. Machine specs

Item	Unit	WT 455
Max. workpiece dimension (W x D x H)	mm	900 × 650 × 245
Max. work piece weight	kgs	550
X travel	mm	450
Y travel	mm	300
Z travel	mm	250
U travel	mm	100
V travel	mm	100
Drive system		AC servo motor
Wire diameter	mm	Ø 0.10 ~ Ø 0.30 (standard)
Machine net weight	kgs	2100
Filter system capacity	L	700
Filter element		Paper filter
Water quality control		Auto
Water temperature control		Auto

$$MRR = \frac{(W1-W2)\times 1000}{\rho \times t} \qquad \text{Eq. (1)} \qquad [14]$$

where W1 and W2 are the weight of the workpiece before and after machining, respectively (grams) Table 5, ρ is the density of the workpiece in (gm/cc), and t is the machining time in minutes, Table 4.

Table 2. Controllable parameters and their levels

S. No	Parameters	Symbol	Level 1	Level 2	Units
1	Arc On time	AON	9	13	µsec
2	Arc Off time	AOF	10	15	µsec
3	Open Voltage	OV	8	10	volt
4	Feed Rate	FR	1	2	mm/min
5	Servo voltage	SV	40	50	volt
6	Wire tension	WT	6	8	N

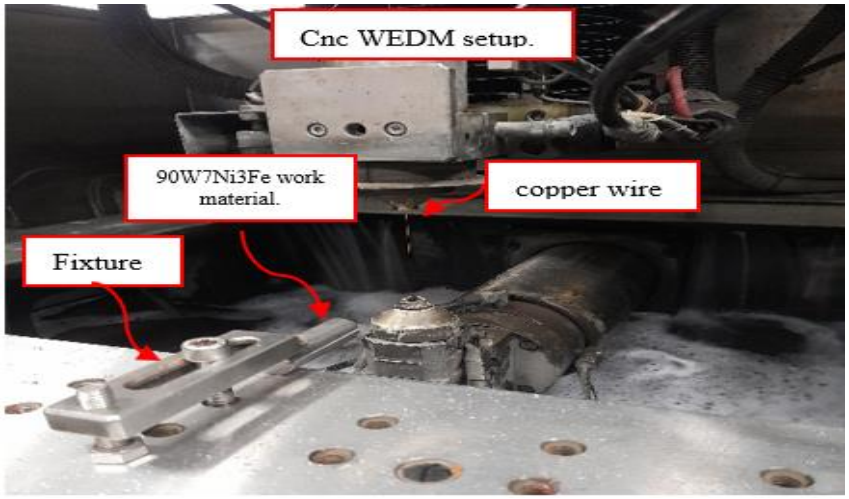

(a)

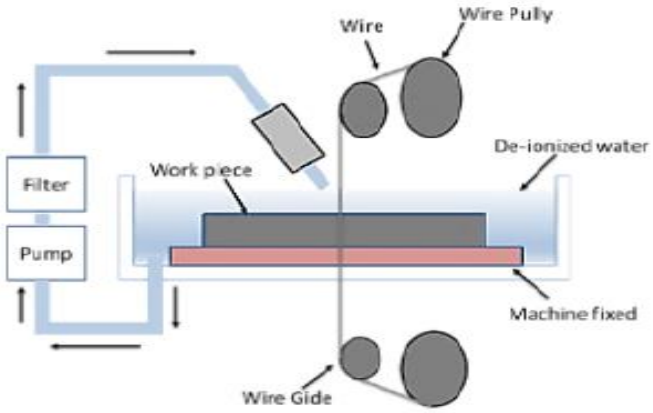

(b)

Fig .1 (a) Actual and (b) schematic Wire electric discharge machining

2.1Cutting mechanism in wire EDM

The material removal mechanism in WEDM (Wire Electrical Discharge Machining) Fig. 2 involves electrical discharges between a wire electrode and the workpiece. As the wire electrode travels along a programmed path, electrical energy is discharged as sparks between the wire and the workpiece [7]. A spark, which cycles a thousand times per second, is created when two electrodes produce a narrow line of molecules. These sparks form the plasma channel between the cathode and anode, producing thermal energy at temperatures between 8,000 ºC and 20,000 ºC to melt and evaporate the substances on the surfaces of each pole [15]. The final stage of WEDM involves continuously bombarding the electrodes with ions and electrons, which leads to extreme heating of the workpiece. The size of the pool of molten metal keeps expanding as the plasma channel widens throughout this phase [16]. A very small portion of the material in the workpiece is removed as molten metal, which eventually solidifies and produces debris. Dielectric fluid removes this material from the discharge zone. Similarly, several craters were observed, giving it a rough, machined appearance [17]. The material removal rate in WEDM depends on several factors, such as the spark gap distance, servo voltage, current density, and wire feed speed. Adjusting these parameters allows the operator to control the material removal rate and produce high-precision and surface finish parts.

2.2 Design of experiment using Half factorial method

The half-factorial technique was used to determine the number of experiments. A powerful and successful design of experiment methodology, the half-factorial method can increase process performance with minimal trials. Rework expenses, production costs, and process cycle times are all decreased. The half-factorial design aims to identify the optimum values for the objective function. The complete design is shown in Table 3.

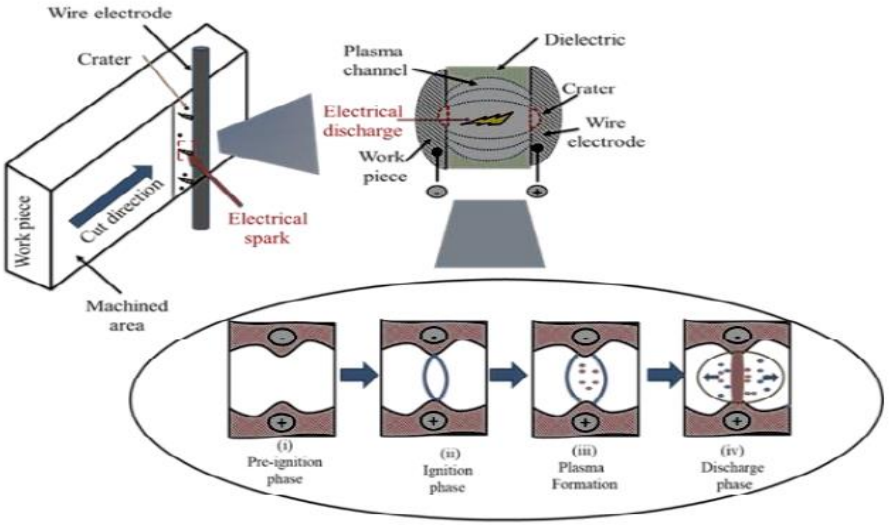

Fig. 2 Spark erosion mechanism in WEDM [7].

Table 3. Design matrix

S.NO	AON	AOF	OV	FR	SV	WT
1	13	10	8	1	40	8
2	13	15	8	2	50	6
3	9	10	10	2	40	6
4	9	15	10	2	40	8
5	13	15	8	1	40	6
6	9	15	8	2	50	8
7	9	10	8	1	50	8
8	13	15	8	2	40	8
9	13	10	10	2	40	8
10	9	10	10	1	50	6
11	9	15	10	1	50	8
12	13	15	10	2	50	8
13	9	15	8	1	40	8
14	9	10	8	2	50	6
15	13	10	10	1	50	8
16	9	10	10	1	40	8
17	9	15	10	1	40	6
18	13	15	8	1	50	8
19	9	10	8	1	40	6
20	9	15	10	2	50	6
21	13	15	10	2	40	6
22	13	10	10	1	40	6
23	13	10	10	2	50	6
24	13	15	10	1	40	8
25	13	10	8	1	50	6
26	9	15	8	1	50	6
27	9	10	10	2	50	8
28	9	15	8	2	40	6
29	13	10	8	2	40	6
30	13	10	8	2	50	8
31	9	10	8	2	40	8
32	13	15	10	1	50	6

3. RESULTS AND DISCUSSIONS OF MRR

Experiments were designed using Half factorial to study the effect of the WEDM process parameter on material removal rate, as shown in Table 4. The average values of material removal rate for each parameter at levels 1 and 2 data are plotted in Fig.3. At a 5% significance level; variance analysis was carried out in the current investigation. ANOVA shows the relationship between the response and the factor with the highest significance rate. This analysis of the 90W7Ni3Fe alloy material removal rate efficiency ANOVA table. The main results of an ANOVA analysis are shown in Table 6. Significant at a 95% confidence level is the MRR for the 90W7Ni3Fe alloy obtained for the Arc on time, Feed rate, Servo voltage, and Open voltage. Therefore, the control parameters are statistically significant, with a confidence level of 95%. The R-sq and R-sq(adj) are 90.37% and 83.42%, respectively.

The proposed suitability of the model was examined using residual analysis. Fig.3 (a). illustrates the residuals, predicted values, and run numbers on a normal probability plot. As the residuals fall in or are very close to the normal straight line, and the divergence from the straight line is minimal, errors are normally distributed. There are no evident patterns or structures in the residuals vs. estimated values and residuals versus run number plots in Figs.3 (b) and (c). It demonstrates that there is no violation of the statistical presumption of independence and constant variance for these experiments and the absence of any residual association. The findings indicate that the suggested model is suitable. The prediction equation for MRR regarding actual factors is expressed as Eq. (2) and is used to predict the response (MRR). It was found that the spark energy will be low for a lower value of AON while the other parameters remain the same, causing less material to be removed, resulting in smaller craters and a finer surface.

A faster MRR was achieved through increased discharge energy and improved Arc on time Fig.4 (a). An increase in the OV value will boost the energy of the pulse discharge, which will, in turn, help the cutting rate. Surface roughness rises with higher open voltage because a higher peak current is produced by higher open voltage. This caused the machining rate to gradually increase along with the surface roughness Fig.4 (c). As feed rate (FR) increases, Ra decreases linearly. With a large rise in material removal rate, surface roughness drastically degrades in this regard Fig.4 (d). The inter-electrode gap that must be maintained during the machining process between the wire electrode and the workpiece is determined by the servo voltage (SV). This is anticipated to impact the concentration of discharge pulses in the machining zone. When the servo voltage increases, the machining rate decreases, and higher levels of debris concentration are seen on surfaces that have been processed at lower servo voltages Fig.4 (e). Arc off time and wire tension had no discernible impact on the material removal rate and other minor factors that were identified to affect surface roughness, as shown in Fig. 4 (b) and (f).

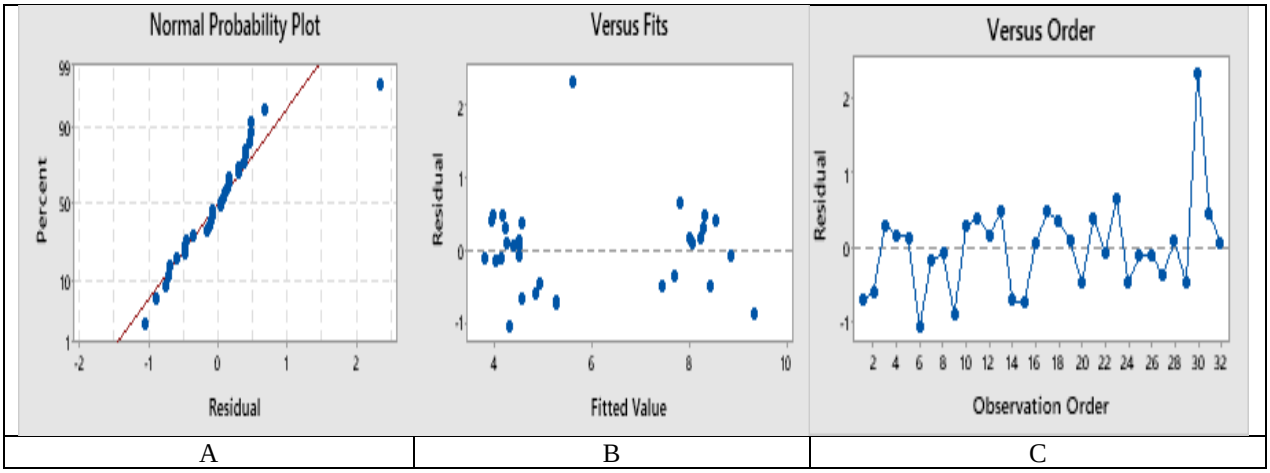

Fig. 3 Residual plot for MRR (a) normal probability plot (b) residual versus fits (c) residual versus order

Table 4. Half factorial experimental design with observed values.

S.NO	Input parameter						Output parameter	
	AON	AOF	OV	FR	SV	WT	Time	MRR
	µsec	µsec	volt	mm/min	volt	N	min	mm3/min
1	13	10	8	1	40	8	15.53	4.562
2	13	15	8	2	50	6	17.11	4.237
3	9	10	10	2	40	6	8.06	8.605
4	9	15	10	2	40	8	8.24	8.191
5	13	15	8	1	40	6	15.41	4.649
6	9	15	8	2	50	8	21.19	3.229
7	9	10	8	1	50	8	18.03	3.864
8	13	15	8	2	40	8	7.49	8.774
9	13	10	10	2	40	8	8.01	8.448
10	9	10	10	1	50	6	15.45	4.513
11	9	15	10	1	50	8	16.5	4.349
12	13	15	10	2	50	8	8.2	8.400
13	9	15	8	1	40	8	16.08	4.452
14	9	10	8	2	50	6	19.3	3.880
15	13	10	10	1	50	8	16.18	4.511
16	9	10	10	1	40	8	16.06	4.451
17	9	15	10	1	40	6	15.55	4.649
18	13	15	8	1	50	8	18.29	4.936
19	9	10	8	1	40	6	16.76	4.318
20	9	15	10	2	50	6	9.29	6.971
21	13	15	10	2	40	6	7.48	8.970
22	13	10	10	1	40	6	15.53	4.433
23	13	10	10	2	50	6	8.02	8.478
24	13	15	10	1	40	8	15.4	4.477
25	13	10	8	1	50	6	17.53	4.027
26	9	15	8	1	50	6	19.06	3.682
27	9	10	10	2	50	8	9.15	7.329
28	9	15	8	2	40	6	8.15	8.180
29	13	10	8	2	40	6	8.51	7.947
30	13	10	8	2	50	8	8.43	7.964
31	9	10	8	2	40	8	7.45	8.793
32	13	15	10	1	50	6	15.06	4.541

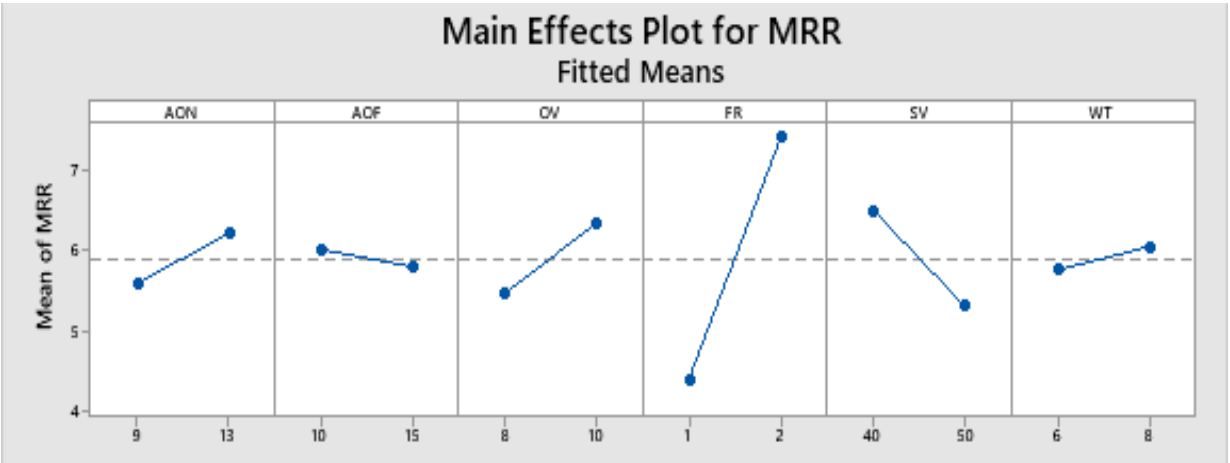

(a) (b) (c) (d) (e) (f)

Fig. 4 Main effect plot for MRR

Table 5. Sample weight before and after the machine

NO	W 1 gram	W 2 gram	NO	W 1 gram	W 2 gram	NO	W 1 gram	W 2 gram	NO	W 1 gram	W 2 gram
1	142.077	140.862	9	63.234	62.073	17	81.609	80.369	25	117.744	116.533
2	150.983	149.739	10	52.741	51.545	18	69.901	68.353	26	106.658	105.454
3	136.713	135.524	11	138.466	137.235	19	58.170	56.929	27	95.842	94.692
4	122.125	120.967	12	160.794	159.613	20	133.877	132.766	28	84.907	83.764
5	107.791	106.563	13	127.051	125.824	21	123.409	122.258	29	74.048	72.889
6	96.913	95.739	14	116.647	115.363	22	112.914	111.734	30	73.407	72.256
7	85.761	84.567	15	105.138	103.886	23	102.844	101.678	31	83.847	82.723
8	74.573	73.446	16	93.648	92.422	24	128.667	127.484	32	93.209	92.036

Regression Equation

MRR = -27.8 + 5.02 AON + 4.96 AOF - 4.17 OV - 0.702 AON*WT + 5.76 FR- 0.537 SV + 8.31 WT - 0.432 AON*AOF + 0.685 OV*FR + 0.0795 OV*SV - 0.1982 FR*SV+ 0.0623 AON*AOF*WT Eq. (2)

Table 6. ANOVA analysis for MRR

Source	DF	Adj SS	Adj MS	F-Value	P-Value
Model	13	114.089	8.7761	13.00	0.000
Linear	6	93.297	15.5495	23.02	0.000
AON	1	3.062	3.0616	4.53	0.047
AOF	1	0.369	0.3688	0.55	0.469
OV	1	5.970	5.9700	8.84	0.008
FR	1	71.953	71.9535	106.54	0.000
SV	1	11.268	11.2681	16.68	0.001
WT	1	0.675	0.6751	1.00	0.331
2-Way Interactions	6	17.683	2.9471	4.36	0.007
AON*AOF	1	0.014	0.0138	0.02	0.888
AON*WT	1	0.760	0.7599	1.13	0.303
AOF*WT	1	0.244	0.2439	0.36	0.555
OV*FR	1	3.749	3.7494	5.55	0.030
OV*SV	1	5.061	5.0608	7.49	0.014
FR*SV	1	7.855	7.8551	11.63	0.003
3-Way	1	3.110	3.1096	4.60	0.046
Interactions AON*AOF*WT	1	3.110	3.1096	4.60	0.046
Error	18	12.156	0.6753		
Total	31	126.246			

R-Sq. = 90.37% R-Sq. (adj) = 83.42%

Conclusion

In this study, the material removal rate and machinability of 90W7Ni3Fe alloy in a wire electrical discharge machine are discussed. The alloy was successfully machined by WEDM. Input process variables were arc on time, arc off time, open voltage, feed rate, servo voltage, and wire tension. According to the investigation, the key factors that influence the rate of material removal are work feed rate, servo voltage, open voltage, and arc on time. According to the results of the half factorial analysis, the best input parameter settings for maximizing the material removal rate are (FR), (SV), (OV), and (AON), in that order. With an accuracy of 90.37%, a regression model was created to predict the MRR. The main result leads to the conclusion that MRR can be increased by raising feed rate, open voltage, and arc on time while lowering servo voltage. The risk of achieving a high Metal Removal Rate value at the expense of sacrificing surface Roughness is significant due to the inverse relationship between Material Removal Rate and Surface Roughness. The work can be improved by discussing the 90W7Ni3Fe alloy's surface roughness during machining, which was not considered in the current study. Multi-objective responses can also be optimized using nontraditional optimization methods including material removal rate and surface roughness.

References

[1] **Niu, L., Jin, Z., Han, X., Zhou, Z., & Guo, J.,2019,** "Modification of tungsten heavy alloy by selective electrochemical etching in sodium carbonate electrolyte", *Journal of The Electrochemical Society*, pp-*166, no*-14.

[2] **Senthilnathan, N., Raja Annamalai, A., & Venkatachalam, G.,2017,** "Sintering of tungsten and tungsten heavy alloys of W–Ni–Fe and W–Ni–Cu: a review", Transactions *of the Indian Institute of Metals*, pp-1161,no-*70*.

[3] **Wei, C., Ye, H., Zhao, Z., Tang, J., Shen, X., Le, G., ... & Le, F.,2021,** "Microstructure and fracture behavior of 90W-7Ni-3Fe alloy fabricated by laser directed energy deposition" Journal of Alloys and Compounds, pp-158975, no-865.

[4] **Jahan, M. P., Rahman, M., & Wong, Y. S.,2011.** "A review on the conventional and micro-electrodischarge machining of tungsten carbide", International journal of machine tools and manufacture, pp-51, no-12.

[5] **Nandam, S. R., Ravikiran, U., & Rao, A. A.,2014,** "Machining of tungsten heavy alloy under cryogenic environment", Procedia *materials science*, pp-296, no-*6*.

[6] **Sagar, C. K., Priyadarshini, A., & Gupta, A. K.,2021,** "Experimental Investigations on The Effect of Tungsten Content on the Machining Behaviour of Tungsten Heavy Alloys", Defence Science Journal, pp-71, no-2.

[7] **Shehata, M., El-Hadad, S., & Attia, H.,2022,** "Wire Electrical Discharge Machining Process: Challenges and Future Prospects", International Journal of Materials Technology and Innovation, pp-31, no-2-2.

[8] **Sathiyaraj, S., Venkatesan, S., & Ashokkumar, S.,2020,** "Wire electrical discharge machining (WEDM) analysis into MRR and SR on copper alloy", Materials Today: Proceedings, pp-1079-1084, no-33.

[9] **Kumar, A., & Singh, D. K.,2012,** "Strategic Optimization and Investigation Effect Of Process Parameters On Performance Of Wire Electric Discharge Machine (WEDM)", International journal of engineering science and technology, no-4.

[10] **Abu Qudeiri, J. E., Mourad, A. H. I., Ziout, A., Abidi, M. H., & Elkaseer, A.,2018, "**Electric discharge machining of titanium and its alloys", The international journal of advanced manufacturing technology, pp-1319-1339, no- 96.

[11] **Abbasi, J. A., Jahanzaib, M., Azam, M., Hussain, S., Wasim, A., & Abbas, M.,2017**, "Effects of wire-cut EDM process parameters on surface roughness of HSLA steel", The *International Journal of Advanced Manufacturing Technology*, pp-1867-1878, no-*91*.

[12] **Raju, P., Sarcar, M. M. M., & Satyanarayana, B.,2014,** "Optimization of wire electric discharge machining parameters for surface roughness on 316 L stainless steel using full factorial experimental design", Procedia Materials Science, pp-1670-1676, no-5.

[13] **Selvam, M. P., & Kumar, P. R.,2017,** "Optimization Kerf width and surface roughness in wire cut electrical discharge machining using brass wire", Mechanics and Mechanical Engineering, pp-37-55, no-1.

[14] **Gaikwad, V., & Jatti, V. S.,2018,** "Optimization of material removal rate during electrical discharge machining of cryo-treated NiTi alloys using Taguchi's method", Journal of King Saud University-Engineering Sciences, pp-266-272, no-3.

[15] **Pramanik, A., (2014),** "Developments in the non-traditional machining of particle reinforced metal matrix composites", International Journal of Machine Tools and Manufacture, pp-44-61, no-86.

[16] **Pramanik, A., & Basak, A. K.,2016,** "Degradation of wire electrode during electrical discharge machining of metal matrix composites", Wear, pp-124-131, no-346.

[17] **Pramanik, A., & Basak, A. K.,2018,** "Sustainability in wire electrical discharge machining of titanium alloy: understanding wire rupture", Journal of Cleaner Production, pp-472-479, no-198.